Solar Energy Advances 3 (2023) 100038

Contents lists available at ScienceDirect

Solar Energy Advances

journal homepage: www.elsevier.com/locate/seja

Testing of uncovered solar thermal collectors under dynamic conditions and identification of performance parameters - for nocturnal radiative cooling applications

Nermeen Abdelnour[a,b,*], Reiner Braun[c,d], Herena Torio[b], Ursula Eicker[d]

[a] Center of Applied Research Sustainable Energy Technologies (zafh.net), University of Applied Sciences Stuttgart (HFT-Stuttgart), Schellingstraße 24, 70174 Stuttgart, Germany

[b] Postgraduate Programme Renewable Energy (PPRE), University of Oldenburg, Carl-von-Ossietzky-Str. 9-11, 26129 Oldenburg, Germany

[c] Reutlingen University, Herman Hollerith Zentrum (HHZ), Danziger Str. 6, 71034 Böblingen, Germany

[d] Dept. of Building, Civil and Environmental Engineering, Concordia University, 1455 Maisonneuve W. Montreal, Quebec H3G 1M8, Canada

ARTICLE INFO

Keywords:
Solar thermal collectors
GenOpt for parameters identification
Collector parameters
Nocturnal radiative cooling
Renewable cooling technologies
Testing standard EN ISO 9806

ABSTRACT

This paper presents the first part of a research-work conducted at the University of Applied Sciences (HFT-Stuttgart). The aim of the research was to investigate the potential of low-cost renewable energy systems to reduce the energy demand of the building sector in hot and dry areas. Radiative cooling to the night sky represents a low-cost renewable energy source. The dry desert climate conditions promote radiative cooling applications. The system technology adopted in this work is based on uncovered solar thermal collectors integrated into the building's hydronic system. By implementing different control strategies, the same system could be used for cooling as well as for heating applications. This paper focuses on identifying the collector parameters which are required as the coefficients to configure such an unglazed collector for calibrating its mathematical model within the simulation environment. The parameter identification process implies testing the collector for its thermal performance. This paper attempts to provide an insight into the dynamic testing of uncovered solar thermal collectors (absorbers), taking into account their prospective operation at nighttime for radiative cooling applications. In this study, the main parameters characterizing the performance of the absorbers for radiative cooling applications are identified and obtained from standardized testing protocol. For this aim, a number of plastic solar absorbers of different designs were tested on the outdoor test-stand facility at HFT-Stuttgart for the characterization of their thermal performance. The testing process was based on the quasi-dynamic test method of the international standard for solar thermal collectors EN ISO 9806. The test database was then used within a mathematical optimization tool (GenOpt) to determine the optimal parameter settings of each absorber under testing. Those performance parameters were significant to compare the thermal performance of the tested absorbers. The coefficients (identified parameters) were used then to plot the thermal efficiency curves of all absorbers, for both the heating and cooling modes of operation. Based on the intended main scope of the system utilization (heating or cooling), the tested absorbers could be benchmarked. Hence, one of those absorbers was selected to be used in the following simulation phase as was planned in the research-project.

1. Introduction

Nocturnal radiative cooling to the night sky is a renewable energy source that can reduce space cooling needs in homes [1]. It is based on the principle of heat loss through long-wave radiation to the cold sky [2]. The potential of radiative cooling depends to a great extent on the local climate conditions [3], as they affect the effective sky temperature [4]. Radiative cooling utilizes the clear night sky as a heat sink [5]. Although this principle goes back to few hundred years BCE, research and development on that topic has flourished only over the past few decades [5–8].

In line with the global transition towards clean and renewable energy sources, environmentally friendly cooling methods are representing an interesting and attractive topic to researchers. However, the available

* Corresponding author at: Center of Applied Research Sustainable Energy Technologies (zafh.net), University of Applied Sciences Stuttgart (HFT-Stuttgart), Schellingstraße 24, 70174 Stuttgart, Germany.

E-mail address: nermeen.abdelnour@hft-stuttgart.de (N. Abdelnour).

https://doi.org/10.1016/j.seja.2023.100038
Received 5 December 2022; Received in revised form 14 May 2023; Accepted 14 May 2023
Available online 16 May 2023

Nomenclature

A	area [m^2]
c_f	specific heat capacity of heat transfer fluid [J/kg.K]
c_1	heat loss coefficient at $(\vartheta_m - \vartheta_a) = 0$ [$W/m^2.K$]
c_2	temperature dependence of the heat loss coefficient c_1 [$W/m^2.K^2$]
c_3	wind speed dependence of the heat loss coefficient c_1 [$J/m^3.K$]
c_4	long-wave irradiance (sky temperature) dependence of the heat losses [-]
c_5	effective thermal capacity [$kJ/m^2.K$]
c_6	wind speed dependence of the zero-loss efficiency $\acute{F}(\tau\alpha)$ [s/m]
E_L	long-wave irradiance [W/m^2]
$\acute{F}(\tau\alpha)$	zero-loss efficiency [-]
G	solar irradiance [W/m^2]
K	incidence angle modifier [-]
$\dot{m}$	mass flow rate of the heat transfer fluid [kg/s]
$\dot{m}_N$	specific mass flow rate [$kg/m^2.s$]
Q	thermal energy (Heat when > 0) [J]
$\dot{Q}$	thermal power [W]
$\dot{Q}_N$	specific thermal power [W/m^2]
T	absolute Temperature [K]
T^*	reduced temperature difference [$K.m^2/W$]
ΔT	temperature difference [K]
t	time [s]
u	wind speed [m/s]

Acronyms

Dev	deviation (an objective function for optimization)
DHW	domestic hot water
HTF	heat transfer fluid
IAM	incidence angle modifier
IR	infra-red
MLR	multiple linear regression
PVT	photovoltaic thermal (hybrid solar collector)
QDT	quasi-dynamic test
RH	relative humidity
SH	space heating
SS	steady-state
STC	solar thermal collector

Greek letters

α	absorptance [-]
ε	emittance [-]
η	efficiency [-]
σ	Stefan-Boltzmann constant (5.67×10^{-8}) [$W/m^2.K^4$]
τ	transmittance [-]
θ	incidence angle of the beam irradiance [°]
ϑ	temperature [°C]

Subscripts

a	ambient Air
b	beam
C	cooling
d	diffuse
en	effective normal
g	global
H	heating
i	inlet
m	mean
o	outlet
s	simulated
sky	sky

literature that tackled radiative cooling go back to the mid-seventies, only. Many of the presented work attempted to predict the effective sky temperature, to eventually estimate the yield of the resource, and also to compare the cooling potential at different locations [3]. Other studies presented theoretical or experimental investigations of radiative cooling systems [2,3,9]. The most recent research on the topic focuses on developing new material to enable daytime radiative cooling [10–12]. Nevertheless, the technology of radiative cooling is still not implemented in conventional buildings. Only for research purposes, special testing systems were designed for measurements and to validate theoretical results (some experiments were carried out in the USA, Jordan, Egypt, and Australia).

Nocturnal radiative cooling systems are similar to solar thermal systems [2,3]. They can be considered as a relatively new technology that can cool surfaces, exposed to the sky during summer nights, exploiting the phenomenon of nocturnal long-wave radiation towards the sky [9,13,14]. Since they are not limited to operate only during summer nights, these systems can be also used for heating applications over day times. By applying a different control strategy, radiative cooling systems can be operated during winter days, to provide both domestic hot water (DHW) and space heating (SH). Radiative cooling systems can hence offer a simple and an affordable solution to reduce power capacity requirements in summer and winter.

Radiative cooling panels are viewed as uncovered flat plate solar collectors [5]. The radiative heat loss from a radiator surface, facing the sky at night, can lower the temperature of the radiator surface and hence the temperature of the heat transfer fluid used in a cooling system. To evaluate the potential use of simple non-insulated thermal collectors, the thermal performance of the collector must first be assessed. This paper focuses on testing some low-cost collectors (e.g. swimming pool absorbers), in order to characterize them thermally with respect to their performance for radiative cooling applications. The outdoors quasi-dynamic test method of the international standard for solar thermal collectors EN ISO 9806 was used in this work as a reference. Thermal characterization of solar collectors is usually done by identifying the thermal performance parameters. To do this, the test database is to be processed using a mathematical optimization tool. In this study, GenOpt was used to optimize and hence to eventually identify the absorbers' parameters. These coefficients of the collector mathematical model are used not only within the simulation environments, but also for plotting the efficiency curves. For radiative cooling systems, this step is essential to evaluate the collector thermal performance, primarily for radiative cooling applications and secondary for heating purposes.

The theory of radiative cooling to the night sky is presented in a glance in the next section. Section 2 (Theoretical Background) also presents the fundamentals needed to understand the principles and operation conditions of solar thermal-collector systems, with the main concern on cooling applications rather than heating. Section 2 ends with a brief of the testing standard. The first part of Section 3 (Methodology) provides an insight into the practical work followed in this research-work. It begins with the testing procedures for some absorbers that are likely to achieve the targeted technical and commercial criteria of this research project. In its second part, Section 3 introduces the mathematical optimization process to identify the absorber parameters, to eventually prepare the mathematical model of the solar absorber. In Section 4 (Results & Discussion), the results of the testing phase are presented. The validation of the optimization model is also discussed. Finally, the parameters of the tested absorbers are presented and used to plot the thermal efficiency curves of the absorbers. The main outcomes and remarks of this work are summarized in Section 5 (Conclusion). It also contains an outlook on the topic "radiative cooling" and recommendations for future research work.

2. Theoretical background

This section aims at providing the fundamentals of radiative cooling-based systems in addition to the basics of modeling solar thermal collectors, and a brief introduction to the testing protocol.

2.1. Radiative cooling

All surfaces emit long-wave radiation and also receive it from their surroundings. The net radiant exchange of energy can result in a significant heat loss of the surface, depending on the temperatures of the surface and its surrounding. Flat plate solar collectors, installed on the roofs of buildings for heating, can act at night as cooling radiators that exchange radiation primarily with the sky [2]. The sky temperature during summer nights can be low enough to result in a net outgoing radiative flux from the collector surface to the open sky, where the sky can be considered as a black body at some equivalent sky temperature T_{sky}, while the flat plate solar collector has a surface emittance ε and a mean temperature T_m [2,3,15]. According to Stefan-Boltzmann law, the actual net radiation between such a horizontal flat plate collector of surface area A, and the sky is giving by Eq. (1), where $\dot{Q}$ is the cooling power and σ is the Stefan-Boltzmann constant, [2,5]:

$$\dot{Q} = A\ \sigma\ \varepsilon\ \left(T_m^4 - T_{sky}^4\right) \tag{1}$$

Thus, flat plate solar collectors can be used for cooling under certain sky conditions, when T_{sky} is low enough to result in a significant cooling power. Indeed, T_{sky} is a key factor that determines the potential for radiative cooling, where T_{sky} is the absolute temperature (in K), and it is raised to the fourth power. It is important to notice that T_{sky} cannot be really measured, it is indirectly calculated, actually. The calculation process of T_{sky} requires having the downward long-wave irradiance from the sky ($E_L \downarrow$) received at the Earth's surface measured. Pyrgeometers at the collector plane are used for this purpose.

For such an untypical mode of operation, the flat plate solar collectors should be called "radiators" rather than "collectors". Yet, this might be confusing, especially when talking about the collector parameters and the testing standard, as will follow in the coming sections. In this paper, however, to distinguish and focus on the cooling operation, collectors will be referred to as "absorbers". In contrast to the conventional operation of solar thermal collectors (STCs), heat losses from the absorber plate are desirable here. Heat loss is the source of the cooling power. Removing the glass cover of the typical STC would immensely allow long-wave radiation emitted from the surface of its absorber plate. Therefore, for radiative cooling applications, unglazed flat plate solar collectors are preferable and the STC consists now of the absorber plate only.

2.2. Convection effect

Having the absorber now directly exposed to the ambient air, convection will also influence the cooling power. However, convection does not always assist in the cooling process. Depending on the local weather conditions (in particular, ambient air temperature and wind speed) and the temperature of the absorber, convection can cause either heat gain or heat loss to or from the absorber surface. If the absorber is warmer than the ambient air, convection will assist in the removal of thermal energy from the absorber. Actually, if ambient air temperature decreases much more rapidly than the temperature of the fluid that is being cooled within the absorber, then much of the cooling effect is the result of convection rather than radiation. And that is actually the case during the first part of the night until about midnight [2,13]. As the absorber surface cools down, the temperature difference between the absorber temperature and the ambient air temperature decreases, and thus the beneficial effects of convection are reduced. If the absorber is colder than the surrounding air, then convective heat exchange counteracts the effects of radiative cooling (i.e. the convection results in heat transfer from the ambient air to the absorber), which is undesirable if the intent is to produce the greatest possible cooling effect [2,13].

This way, the ambient air temperature T_a affects the operation of night-cooling in two ways: primarily affecting the radiative part of the heat exchange (indirectly in the calculation of T_{sky}), and secondarily in the form of convective heat losses or gains, which can significantly enhance or lower the performance of the cooling-absorbers. In a nutshell, the weather conditions which have to be taken into account, when considering the potential analysis for night-cooling applications, are [2,3,13]:

- The ambient dry bulb temperature
- The relative humidity
- The effective nocturnal sky temperature
- The wind velocity

2.3. System technology

Roof-mounted STCs have been used since several decades to provide DHW for residential buildings, mainly in Europe, Australia, and USA [2,15]. Nevertheless, the heat transfer fluid (HTF) can also be used to support low-temperature heating systems [2,16]. The SH concept can be applied by circulating the HTF through a hydronic system integrated within the conditioned spaces of the building [2]. The same idea could be used during summer nights to cool down the HTF, harnessing the night-cooling principle as explained in the previous sections [2,16]. In either case, the STC is the key component of the system, where it generates thermal energy, whether heat or cold.

2.3.1. Mathematical model

To predict the annual energy yield a solar thermal system can produce, it is important to know the thermal performance of a STC [17]. The modeling of a STC is based mainly on its common mode of operation, i.e. for heating purposes. Different mathematical models are used to characterize liquid heating STCs, depending on their type (glazed or unglazed) and the test method used (steady-state (SS) or quasi-dynamic test method (QDT)) [18]. The SS method does not account for the diffuse irradiance. Moreover, there is no parameter to account for sky temperature dependency (instead, an equivalent net irradiance is calculated in SS) [17,18]. For unglazed STCs, the most important heat loss terms are the wind speed dependencies, and as explained earlier, there is a significant effect due to exchange with the sky in long-wave radiation (the infra-red (IR) range). Using the complete model of STCs, which is based on the QDT method, is therefore mandatory for unglazed collectors [17,18]. This is provided by the international standard for solar thermal collectors EN ISO 9806. The latest update of the standard (ISO 9806:2017) paid due attention to unify the description, as well as the presentation of the results, of the thermal performance regardless of the collector type and test method. The same was considered for the description of the incidence angle correction factor [19]. In this work, the full model of STCs based on the quasi-dynamic test method (QDT) of the ISO 9806:2013 was used. This model is in line with the newest version proposed in the ISO 9806:2017. Discrepancies between both versions of the standard are discussed at the end of this section. The energy balance equation, in the quasi-dynamic approach according to the international standard for solar thermal collectors EN ISO 9806:2013, is expressed as:

$$\begin{aligned}\dot{Q}_N = {} & F'(\tau\alpha)_{en}K_b(\theta)G_b + F'(\tau\alpha)_{en}K_dG_d \\ & -c_1\left(\vartheta_m - \vartheta_a\right) - c_2\left(\vartheta_m - \vartheta_a\right)^2 \\ & - c_6u\,G_g - c_3u\left(\vartheta_m - \vartheta_a\right) \\ & +c_4\left(E_L - \sigma T_a^4\right) \\ & -c_5\frac{d\vartheta_m}{dt}\end{aligned} \tag{2}$$

Eq. (2) was intentionally written in such a way in order to group the heat-loss terms according to the heat transfer mechanism responsible for their occurrence: conduction, convection, or radiation. The terms and coefficients in the equation are explained below [17,18,20]:

- G_b & G_d: are the beam and diffuse solar irradiance, respectively [W/m^2]. They represent the input energy in the heating mode, and they are equal to zero during night operation.
- $K_b(\theta)$ & K_d: are the incidence angle modifier (IAM) for beam and diffuse radiation, respectively [-]. The IAM is to define the efficiency at any given incidence angle θ.
- $(\tau\alpha)$: is the transmittance-absorptance product of the collector cover [-]. This product should account for the effective value on the collector plane $(\tau\alpha)_e$, but if the IAM is introduced in the equation (like in Eq. (2)), then this product can be replaced by the value at normal incidence $(\tau\alpha)_{en}$, which is more convenient to provide as a collector constant.
- F': is the absorber efficiency factor [-].

The product $F'(\tau\alpha)$ corresponds to the zero-loss efficiency (or the so-called conversion factor η_o in some literature and actually in the newest standard). Heretofore, the first two terms of Eq. (2) represent the absorbed solar energy by the collector. However, it is not fully converted into useful heat energy. There are different environmental heat losses that occur at the absorber surface. Such losses are expressed by the other six terms in the equation, as following [17,18,20]:

- c_1: is the heat loss coefficient at $(\vartheta_m - \vartheta_a) = 0$ [W/m^2.K], where ϑ_m is the absorber mean temperature and ϑ_a is the ambient air temperature.
- c_2: describes the temperature dependence of the heat loss coefficient c_1 [W/m^2.K^2].

Those two collector parameters (c_1 and c_2) express the "conduction and natural convection losses" of the absorber.

- c_3: describes the wind dependence of the heat loss coefficient c_1 [J/m^3.K].
- c_6: describes the wind dependence of the zero-loss efficiency [s/m], and G_g is the incident global solar irradiance.

The dependency of those two parameters c_3 and c_6 on the wind speed u introduces their corresponding terms in the third line of the energy balance equation as "forced convective heat losses".

- c_4: describes the long-wave irradiance (sky temperature) dependence of the heat losses [-].
- E_L: is the measured long-wave thermal irradiance at the collector plane [W/m^2].
- σ is the Stefan-Boltzmann constant [W/m^2.K^4].
- T_a is the absolute ambient air temperature [K].

The net long-wave irradiance $(E_L - \sigma T_a^4)$ is added to the equation in order to express the heat loss dependence on long-wave irradiance (i.e. radiative losses), taking the emittance-absorptance ratio (ε/α) of the absorber plate into account as a correction factor (where the collector parameter c_4 is equivalent to the (ε/α)-ratio). Normally the value of $(E_L - \sigma T_a^4)$ is a negative value, as the effective sky temperature ($E_L \downarrow = \sigma T_{sky}^4$ [2]) is lower than the ambient air temperature.

- c_5: is the effective thermal capacitance of the collector [J/m^2.K].

It is an important parameter when it comes to dynamic system simulation, as it describes the transient behavior of the collector. Unfortunately, the effective thermal capacity depends on the operating conditions and is not a collector parameter with a constant value [20].

Finally, when all those possible losses are deducted from the absorbed solar energy as in Eq. (2), this leads to the specific useful power output of the collector $\dot{Q}_N$ [W/m^2]. On the other hand, $\dot{Q}_N$ can also be expressed as a function of the fluid mass flow rate $\dot{m}$, the specific heat capacity c_f, the temperature difference ΔT between the fluid outlet and inlet $(\vartheta_o - \vartheta_i)$, and the absorber area A, as given by Eq. (3):

$$\dot{Q}_N = \dot{m}\, c_f\, \Delta T / A \tag{3}$$

For radiative cooling applications, $\dot{Q}$ is a cooling power (i.e. of a negative value). Although the solar irradiance components G_b and G_d are zeros in the cooling mode (night operation), it is important to explicate the full collector mathematical model as per Eq. (2), because it is the basis for the testing protocols, as will follow in Section 3 (Methodology).

In the ISO 9806:2017, a slightly different model fitting for the so-called WIS-Collectors (Wind Infra-red Sensitive - collectors) is included. Where the reduced wind speed u' $(u - 3$ m/s) is used in the equation instead of u. And two more heat loss coefficients are considered, namely c_7 (the wind dependence of the infra-red (IR) radiation exchange) and c_8 (the radiation losses) [19]. Noting that, the eight heat loss coefficients are denoted in that latest revision of the standard by the letter a not c. Worthy to mention is that, coming back to the previous model (for the thermal performance) as adopted in the version of 2013 is under discussion in the ongoing revision of the standard [21].

2.3.2. Design characteristics

For night cooling applications, optimum performance is achieved by maximizing the heat losses out of the solar absorber. The only term in Eq. (2) that always ensures a "heat loss" is the radiative losses term (of the coefficient c_4). The other terms in the equation may cause heat loss or gain, depending on the absorber mean temperature (ϑ_m) with respect to the ambient air temperature (ϑ_a). Therefore, radiative cooling applications require special construction as well as design criteria of the solar absorber. The goal is to allow maximum heat loss by long-wave radiation towards the sky [9].

In terms of construction, the uncovered design is chosen. Furthermore, backside insulation is to be evaluated, as it might help in the heat removal process by convection. On the system level, it is recommended to shade the absorber field during the daytime, as a means of thermal insulation to reduce the undesirable solar gains [2]. Providing shading to the absorber field does not sound practical and is not always easy to implement, in addition it can be costly. The optical properties, as a design parameter, could be an alternative.

Typically, a solar absorber should have a selective surface where the absorber surface has high absorptance at the visible spectrum (short wavelengths), to capture the solar irradiance, and low emittance at the IR spectrum (long wavelengths), to minimize heat loss via radiation [22]. Contrariwise, when the thermal system is designed mainly for cooling purposes, the solar absorptance (α) is of little importance [2]. It can have low values which helps in reducing solar gains during daytime on the one hand and increases (ε/α)-ratio on the other hand. The (ε/α)-ratio is defined as: the ratio of infra-red emittance of a material to its absorptance in the short-wavelength range of solar radiation. The radiative heat loss coefficient c_4 in Eq. (2) is the optical parameter (ε/α)-ratio of the absorber [18]. To achieve high absorber cooling efficiency, it is preferable to have a high IR emittance (ε), as it maximizes the heat removal through radiation. Depending on the application of the solar thermal system, the design of the optical properties differs. For nocturnal radiative cooling applications, it is better to have high values of (ε/α)-ratio (c_4). Nevertheless, such a design criterion lowers the heating efficiency if the system works in a dual-mode operation.

The recently published articles in the topic of radiative cooling pay due attention to optical properties [11]. Modern technologies [8] and advanced materials [10,12] to manipulate solar radiation were investigated. The focus was on daytime radiative cooling, however [6,7,23].

In this work, a number of plastic absorbers of different designs are tested. The tested absorbers were selected from the available range of swimming pool absorbers in the European market. Worthy to mention is that, for applications focused on radiative cooling, the absorber material should be treated first to improve the optical properties, as explained above. Moreover, the material should have a reasonable thermal con-

ductance to allow for as much heat transfer as possible from the HTF. Nevertheless, very good contact between the HTF and the entire (inner) surface of the absorber plate (or tubes) results in almost a similar (cooling) performance as in the case with materials of high thermal conductivity, like the commonly used metallic absorbers [2]. The mass flow rate of the HTF plays an important role in this respect.

2.3.3. Operation parameters

The rate at which the HTF is forced to flow through the absorber affects the cooling performance of the system. As understood from Eq. (3), at any realized cooling (or even heating) power ($\dot{Q}_N$), high mass flow rates ($\dot{m}_N$) result in low temperature differences (ΔT), whilst a significant ΔT is achieved by a low $\dot{m}_N$. However, to fulfill the condition of maximizing the surface contact area as explained above, it is important to comply with the manufacturer's recommended specific mass flow rate, to ensure the desired heat transfer from the HTF to the absorber surface. Nevertheless, after sizing one absorber module, the layout of the absorber field (series or parallel connection) can manipulate such a restriction based on the application requirements [24].

For the testing part in this research-work, a water-glycol mixture was used as the HTF (1/3 of Ethylene glycol, $C_2H_6O_2$, melting-temperature −13 °C [25]). A pump is necessary in radiative cooling systems, because usually the temperature difference between the absorber inlet and outlet is not large enough to initiate thermosyphon circulation [13].

2.4. Testing standard

The international standard EN ISO 9806:2013, that was available while conducting this work, specified test methods for the thermal performance characterization of fluid heating collectors [18]. The test database is to be used then within a parameter identification process to identify the full performance parameters. Those coefficients are also used to plot the thermal efficiency curves for heating and cooling. Based on the main scope of the system utilization- heating or cooling, the absorber thermal performance can be evaluated.

The test conditions, requirements, procedure, as well as the description of the test sequences are well explained in the standard [18]. The main criteria for quasi-dynamic testing are listed in the Appendix.

3. Methodology

This section introduces the practical work followed in this project to eventually define the mathematical model of the absorbers under testing, as presented in the previous section. It begins with the testing procedures. Then, it presents the mathematical process to identify the absorber parameters.

3.1. Testing overview

The test facility at HFT-Stuttgart is especially prepared for testing and characterization of solar collectors. It is an outdoors test-stand on which up to five collectors can be tested simultaneously under dynamic conditions. Simultaneous testing does not only save testing-time, but it also assures undergoing same testing conditions, in addition to the possibility of direct comparison of the results [16]. In this project, five plastic solar absorbers of different designs were tested. The first absorber (SunSet) and the second (AQSol) had a wooden plate on the back-side. They had also a similar design of thin tubes. Their gross areas were 2.77 and 1.8 m^2, respectively. For technical reasons, it was decided to disregard the third absorber on the test-stand. The forth absorber (Solar-Ripp) had also a wooden plate on the back. However, there was a thin air-gap in between, due to the corrugated design of its thick tubes. Its gross area was 1.72 m^2. The fifth absorber (ROTH) had a flat area of 2.2 m^2, with no plate-covering at all. The Appendix encloses a photo of the tested absorbers on the test-stand as well as the datasheets of the four tested absorbers. The technical specification of a solar thermal absorber does not often include the complete set of the parameters described in the QDT-based model. But in order to configure the solar absorber as a system-component in simulation programs, all parameters included in the absorber mathematical model have to be provided as inputs. Consequently, a parameter identification process has to be carried out for any absorber in preparation for any probable simulation phase. This process implies testing the absorber for its thermal performance.

3.1.1. Test set-up & procedures

The testing procedure was developed based on the QDT method of the EN ISO 9806:2013. The challenge in QDT is to ensure large enough variability in solar radiation during the test [18]. A wide range in inlet temperatures is furthermore essential in order to decouple thermal and optical parameters [20]. That was achieved through real-time recording of the test data. To comply with the QDT requirements, all measurements were logged every 10 s [16,18]. An Ahlborn Almemo 5590–2 data logger and the software LabVIEW were used for that purpose. And to achieve suitable test data, a reversible chiller (with variable temperature control from −20 to 60 °C) was also used to control the inlet temperature to the absorbers. The used Huber unichiller 100T-H8-TP35W0 is able to stabilize the set temperature within ±0.2 °C. Moreover, it was upgraded, by a special control feature, to be able to regulate the inlet temperature as a function of the ambient temperature in the range of ±30 °C. This feature helps in achieving a wide range of inlet temperatures during the test period. Fig. 1 shows the basic idea of communication and data acquisition to generate the measurements data files.

3.1.2. Measurements

The useful thermal power output of each of the four absorbers was calculated from the measured volumetric flow rate and the tempera-

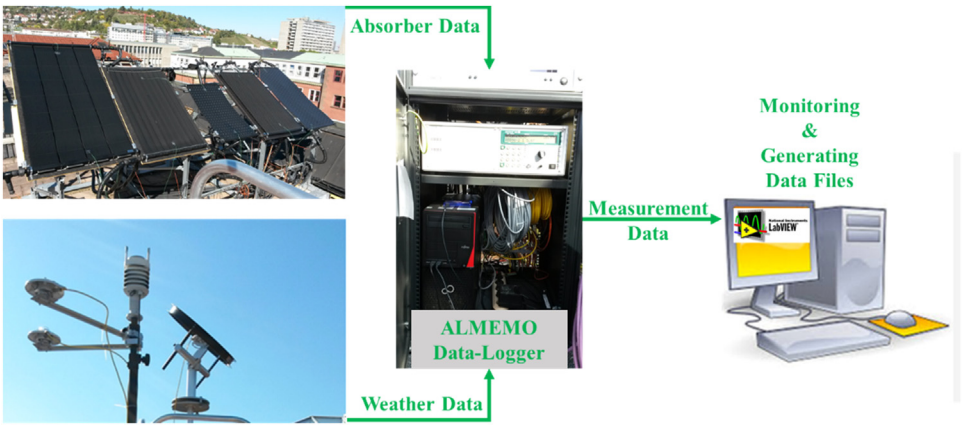

Fig. 1. The concept of data acquisition of the measurements at the test facility at HFT-Stuttgart.

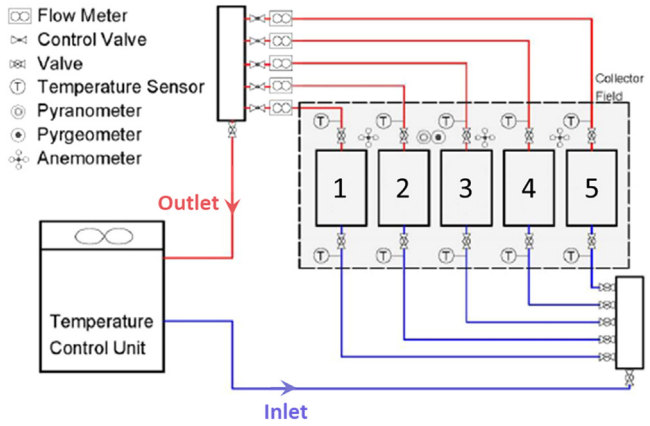

Fig. 2. The hydraulic scheme of the absorbers on the test-stand.

ture difference between the inlet and outlet of the absorber, according to Eq. (3). On the absorber plane, the wind speed, global solar irradiance, and long-wave irradiance were also measured. Fig. 2 shows the hydraulic scheme of the absorbers on the test-stand. It also indicates the position of the tested absorbers, temperature sensors, measurement devices and control valves. Furthermore, a weather station was provided at the test facility for the measurement of the global and diffuse solar irradiance as well as the long-wave irradiance, on the horizontal plane. The horizontal diffuse radiation was measured with a pyranometer equipped with a shadow-ring. Table 1 lists the measuring devices installed at both the test-stand and weather station indicating their main specifications.

3.1.3. Test period

After the complete set-up of the absorbers on the test-stand, the hydraulic circuit was connected. The whole system was inspected and tested for reliable data recording. It is defined by the standard that the test period consists of 4–5 sequences. A test sequence is the time interval during which data would be considered in the analysis phase (which will follow for the parameter identification process). The minimum length of a test sequence shall be 3 h. The 3 h do not need to be consecutive (the test sequence can consist out of several non-consecutive parts) [18]. Certain weather conditions are required during the test period. Thus, the number of actual testing days is dependent on the actual weather conditions on the test site. Therefore, the testing phase can take long time. In this work, the testing phase was conducted in November and December which were assigned considering the project timeframe. The test conditions, requirements, procedure, as well as the description of the test sequences are explained in the standard in detail [18]. The main criteria for quasi-dynamic testing are summarized in the Appendix. Generally, clear sky as well as partly cloudy conditions are needed in quasi-dynamic testing for accurate determination of parameters [18]. The inlet temperature for the four absorbers was adjusted on the test days trying to fulfill the requirements as stated in the standard. Somedays ϑ_{in} was set at a constant value and some other days it was set as a function of the ambient temperature. The specific mass flow rates for the four absorbers were regulated according to the manufacturers' recommendation. In general, $\dot{m}_N$ ranged between 100 and 150 kg/m^2.hr. Sufficient data has been recorded over the two months testing period. This data was evaluated for each day. Despite the large test database, only three days by the end of December were the best that nearly met the testing criteria of quasi-dynamic testing. The main measurements on those days (the 19th, 22nd and 26th) are plotted on Fig. 3. A test sequence from 10:00 h till 16:00 h was selected on each of those three test days. The cascaded test sequences were to be processed in preparation for the parameter identification process. The inlet temperature on those three selected days was set at 16 °C, ϑ_a, and ϑ_a, respectively. Interestingly, it can be noticed on plots (b) and (c) of test days 2 and 3 respectively (when $\vartheta_{in} = \vartheta_a$) that at nighttime the mean fluid temperatures of the four absorbers go below the ambient temperature. This is due to radiative heat losses to the cold sky. The sky temperature reached −10 °C on test day 3, for example, while the ambient temperature barely dropped to 8 °C. Further analysis and additional figures plotting ϑ_{sky} are included in the Appendix. Table 2 presents the main statistical values for the important measured data on those three days (during the predefined test sequence). Worthy to mention is that, testing in summer would have been preferable (for this specific experiment in Stuttgart) to shorten the overall testing period from one hand, and to offer more suitable test data from the other hand. The number of test days (and hence test-sequences), that could be considered for further analysis, depends on the suitability of test data [18]. On the other hand, it is important to highlight that nighttime tests are not yet included in the standard [21].

3.2. Parameter identification process

To identify the collector parameters, the international standard ISO 9806:2013 proposed the non-iterative mathematical method - Multiple Linear Regression (MLR). However, other non-linear methods can be used as a parameter identification tool, provided that they are minimizing the error in the output power of the collector as in the MLR method [18]. The dynamic parameter identification has been widely used with promising results [17]. Dynamic parameter identification is a non-linear method to find the best fit of a given parameterized model to a real system based on a time sequence of some measurable output. The best fit is given by the set of parameter values, which minimizes an objective function. The objective function, in principle, is the integral of the root mean square of the difference between the measured and simulated values. The minimum of the objective function is searched in an iterative process [17].

3.2.1. GenOpt

GenOpt is a generic optimization program developed to automatically determine the optimal parameter settings for system optimization. It is a dynamic optimization tool that uses mathematical programming to find the values of user-selected design parameters that minimize a pre-defined objective function. The objective function is evaluated by a simulation program that is iteratively called by GenOpt [26].

For the identification of the parameters of the four absorbers under testing, GenOpt was coupled to TRNSYS17, and Hooke-Jeeves optimization algorithm was implemented [26]. A simulation model was developed to serve as an optimization template for each of the four absorbers.

Table 1
The main specifications of the measurement devices installed at the test facility at HFT-Stuttgart for collectors' characterization.

Measured Quantity	Sensor	Range	Accuracy
Fluid Temperature	Temperature Sensor (Pt100 1/3 class B)	–	0.1 + 0.005T °C
Volumetric Flow	Flow Meter Magnetic inductive flow sensor (SIKA VMZ081)	0.25 - 5 l/min	±1%
Global Solar Irradiance (On the absorber plane)	Pyranometer (Huskeflux SR20)	n/a	±1%
Long-wave Irradiance (On the absorber plane)	Pyrgeometer (Huskeflux IR20)	n/a	4.5%
Solar Irradiance (Global & Diffuse) (On the horizontal plane)	Pyranometer (Kipp&Zonen CMP21)	285 to 2800 nm	±1.4%
Long-wave Irradiance (On the horizontal plane)	Pyrgeometer (Kipp&Zonen CGR 4)	4500 to 42,000 nm	
Wind Speed	Anemometer (Cup Anemometer Wilmers Messtechnik)	0 - 10 m/s	±0.3 m/s

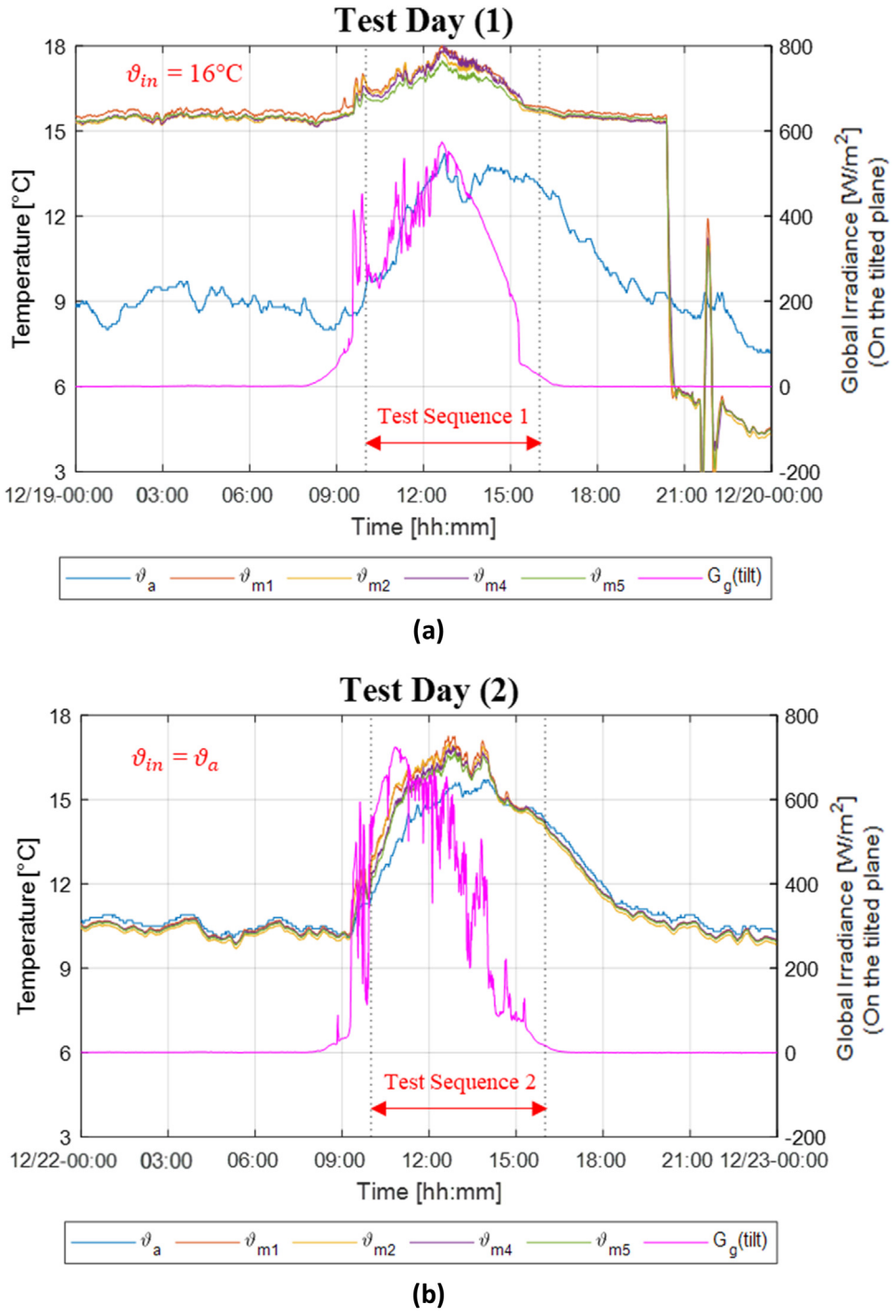

Fig. 3. The weather conditions and the mean fluid temperatures of the four absorbers on the three testing days for parameter identification.

The objective function was defined as the deviation between the measured and simulated outputs. In particular, the fluid outlet temperature, as indicated in Eq. (4), where "Dev" is the objective function to be minimized, $\vartheta_{os,i}$ and $\vartheta_{o,i}$ are the simulated and measured temperatures outlet from the absorber, respectively.

$$Dev = \sum_{i=1}^{n} \sqrt{\left(\vartheta_{os,i} - \vartheta_{o,i}\right)^2} \quad (4)$$

To perform the optimization, GenOpt automatically generates input files for the simulation program. These files are based on the TRNSYS input template (a parameterized absorber model). GenOpt then launches the simulation program, reads the function value being minimized from the simulation result file. Subsequently, it checks possible simulation errors and then determines a new set of input parameters for the next run. The whole process is repeated iteratively until a minimum of the function is found [26]. Fig. 4 describes this iterative process.

3.2.2. Optimization template

Fig. 5 shows the template of TRNSYS simulation model that was developed to optimize the absorber's parameters. Type1289-Unglazed from TESS solar library models uncovered solar collectors and uses the dynamic efficiency approach of the earlier version of the Standard (EN12975), i.e. the complete set of parameters is used to model the STC component [27]. It was therefore suitable to simulate the absorbers un-

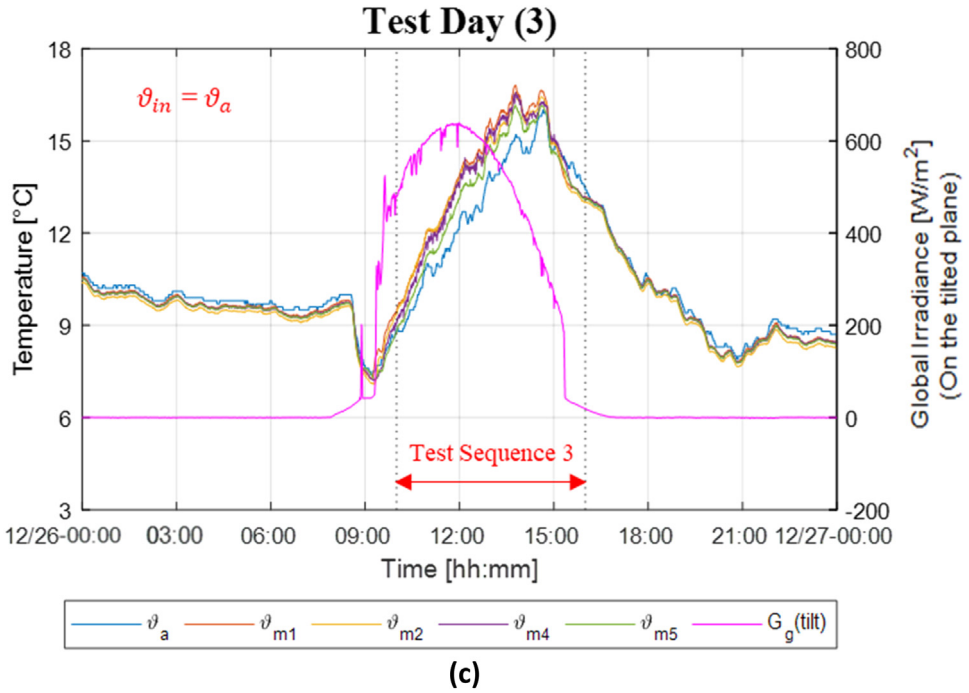

Fig. 3. Continued

der testing. This simulation model was coupled with GenOpt to identify the absorber parameters through the optimization process. The seven coefficients in the absorber mathematical model ($F'(\tau\alpha)$, c_1, c_2, c_3, c_4, c_5, c_6) were parameterized while configuring the absorber component (Type1289). Whilst all other required inputs and parameters were provided from the data files that were generated from the measurements as indicated on Fig. 1.

4. Results & discussion

For each of the four absorbers under testing, the corresponding data files ("Collector" and "Weather") on the three selected test days, were imported in the simulation model template, as indicated in Fig. 5. Then, GenOpt was coupled with that template input file. By running the GenOpt configuration file, an iterative process for the seven parameterized variables took place. The process ends when the pre-defined objective function reaches its minimum. The time required to complete the optimization was less than one hour for each absorber. The results of the optimization process are listed in Table 3. The heat loss coefficient c_1 of the first two absorbers has the lowest values due to the tight back cover. Although absorber 4 has also a back cover, it has the highest value of c_1. This is due to the thin air-gap it has from the back (s. Section 3.1). Absorber 5 has the highest wind dependence factor c_3 of the heat loss coefficient c_1. This is mainly because of the vast exposure to the wind from both the front and back sides. Worthy to mention is that the wind dependence factor c_6 of the zero-loss efficiency of all absorbers (except absorber 4) could not really be identified. The value 0.0005 was actually the minimum limit that was set to that parameter in GenOpt during the optimization process.

4.1. Model validation

In order to ensure the quality of the identified parameters, both the fluid outlet temperature and the absorber output power were calculated on the test days using the values of the identified parameters in the same simulation model template (Fig. 5). The measured inlet temperature from the test stand served as an input to the TRNSYS model. Those two simulation-based results were compared to the measured data on

Table 2
Conditions during the selected sequences on the three testing days.

		Mean	Min.	Max.	Standard Deviation
Weather Station Data					
Ambient temperature (ϑ_a) [°C]		13.36	8.80	16.00	1.70
Wind speed (u) [m/s]		0.41	0.00	1.83	0.36
Global solar irradiance (G_g) on the tilted plane [W/m²]		399.53	16.65	723.25	208.00
Sky temperature (ϑ_{sky}) [°C]		−5.14	−9.24	4.60	2.39
Absorbers Test-stand Data					
Absorber 1	Temperature difference ($\vartheta_m - \vartheta_a$) [°C]	2.12	−0.82	6.73	1.84
	Mass flow rate [kg/m².hr]	120.85	112.85	127.42	2.97
Absorber 2	Temperature difference ($\vartheta_m - \vartheta_a$) [°C]	2.00	−0.95	6.66	1.85
	Mass flow rate [kg/m².hr]	119.03	111.08	125.68	3.04
Absorber 4	Temperature difference ($\vartheta_m - \vartheta_a$) [°C]	1.95	−0.76	6.59	1.84
	Mass flow rate [kg/m².hr]	123.66	103.33	146.51	13.53
Absorber 5	Temperature difference ($\vartheta_m - \vartheta_a$) [°C]	1.69	−0.76	6.38	1.82
	Mass flow rate [kg/m².hr]	143.88	136.54	149.34	3.99

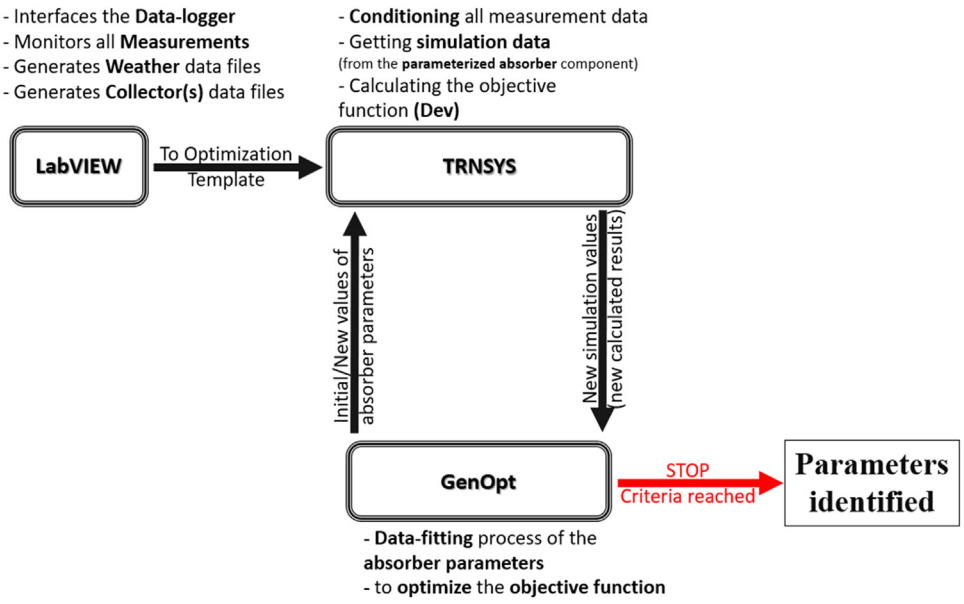

Fig. 4. The principle in identifying the absorber parameters.

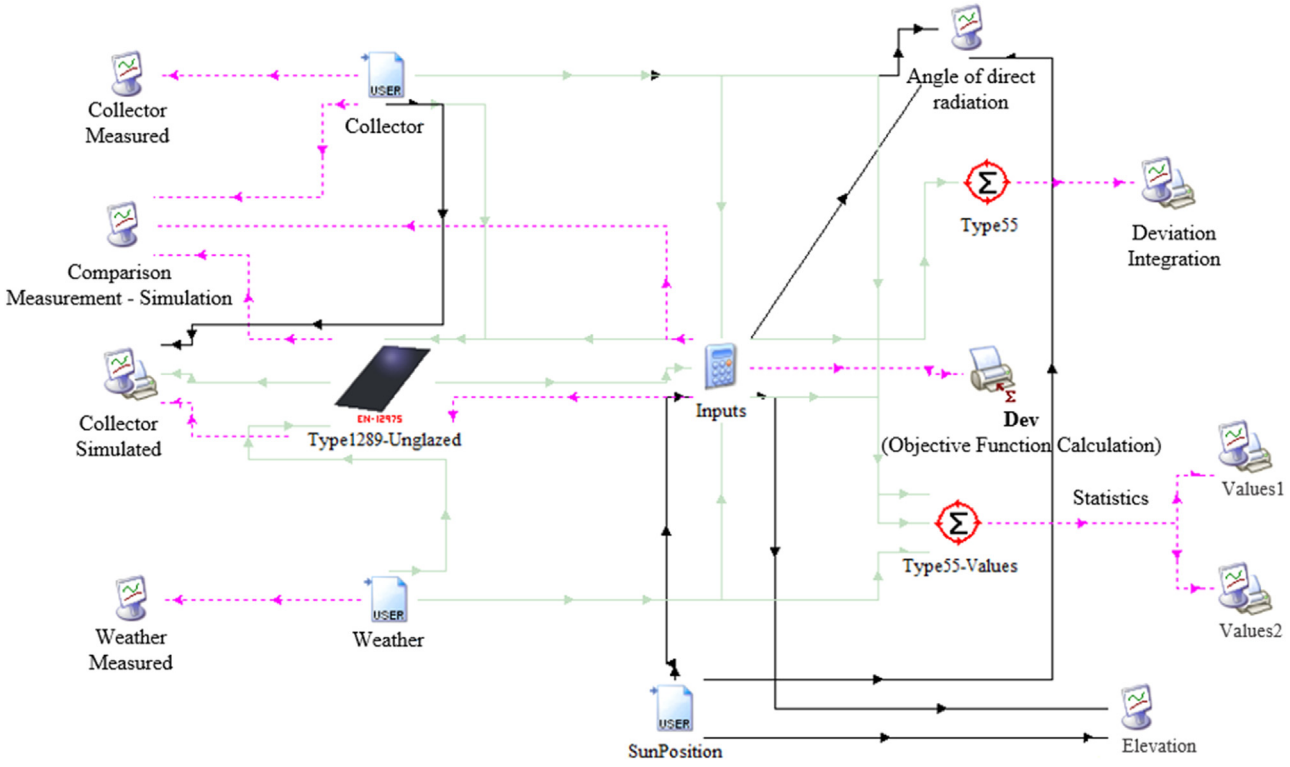

Fig. 5. TRNSYS model that was coupled with GenOpt serving as the optimization template (in which the absorber Type1289 was parameterized).

Table 3
The identified parameters (and areas) of each of the four tested absorbers.

	Absorber 1 SunSet	Absorber 2 AQSol	Absorber 4 Solar-Ripp	Absorber 5 ROTH	Units
Absorber area A	2.77	1.80	1.72	2.20	[m^2]
Zero-loss efficiency $F'(\tau\alpha)$	0.83	0.87	0.89	0.76	[-]
Absorber heat loss coefficient c_1	7.68	7.01	13.96	10.85	[$W/m^2.K$]
c_1-temperature dependence c_2	0.00014	0.00014	0.00375	0.00278	[$W/m^2.K^2$]
c_1-wind dependence c_3	3.70	7.35	4.05	13.85	[$J/m^3.K$]
Long-wave irradiance dependence c_4	0.365	0.71	0.515	0.64	[-]
effective thermal capacitance of the absorber c_5	13.25	17.30	59.25	31.85	[$kJ/m^2.K$]
Wind dependence of the zero-loss efficiency c_6	0.0005	0.0005	0.0275	0.0005	[s/m]

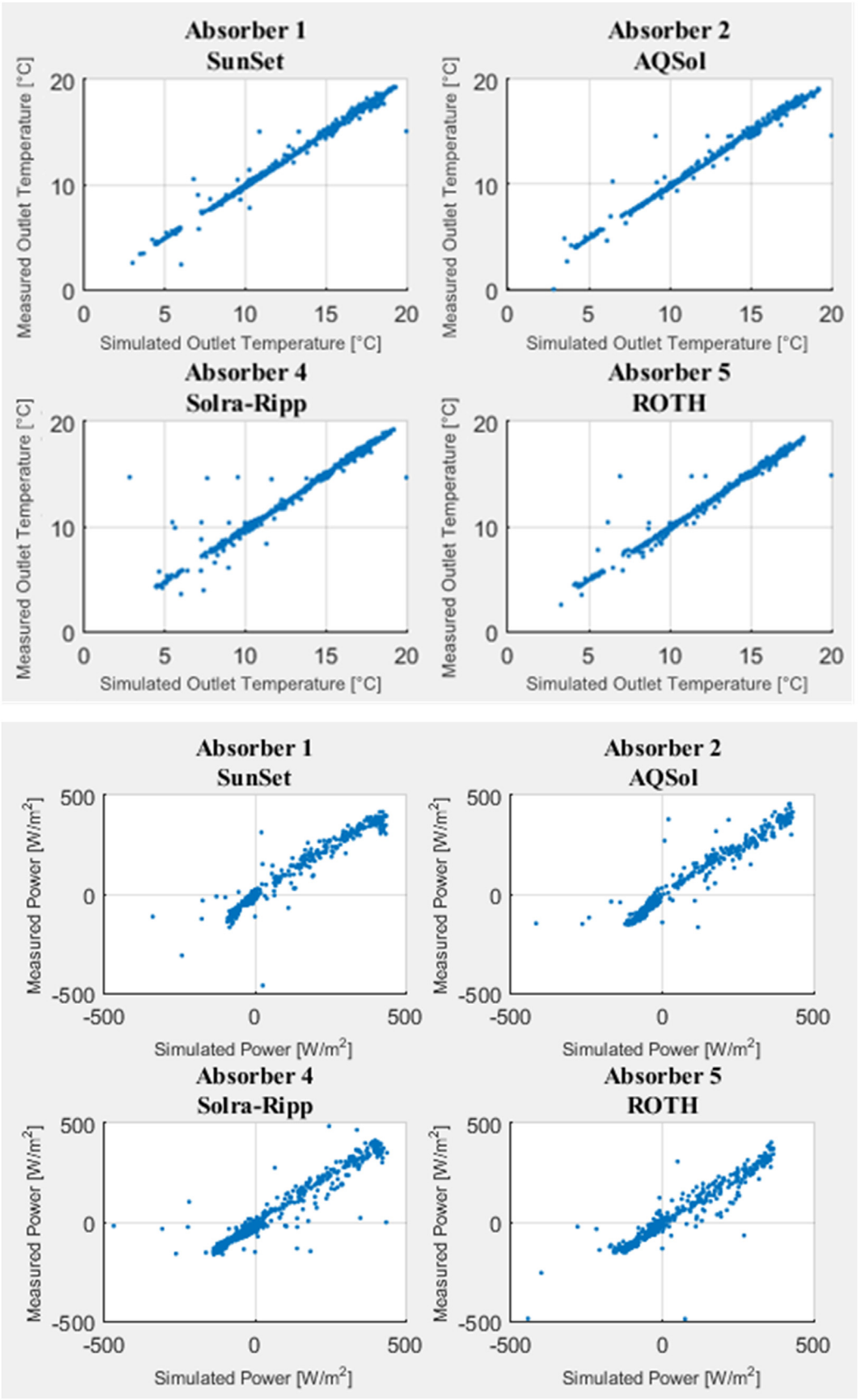

Fig. 6. Comparison between the simulated and the measured values of the fluid outlet temperature (top) and the specific power output from the absorber (bottom) on the three test days.

Table 4
Statistical analysis to benchmark the simulated values to the measured data.

	$\vartheta_{os} - \vartheta_o$ (in °C)		$\dot{Q}_{Ns} - \dot{Q}_N$ (in W/m²)	
	Mean	Standard deviation	Mean	Standard deviation
Absorber 1 (SunSet)	0.12	0.37	14.51	38.79
Absorber 2 (AQSol)	0.19	0.39	21.41	50.82
Absorber 4 (Solar-Ripp)	0.12	0.67	13.98	77.22
Absorber 5 (ROTH)	0.09	0.44	11.98	59.31

the same days. As shown in Fig. 6, the plots show a good match between the simulated and measured values. The negative values of the output power (graphs at the bottom) mainly represent the night data of the three test days. This accounts for the night-cooling phenomenon when the fluid was cooled down. Table 4 presents the mean and standard deviation of the difference between the simulated and measured values for both the fluid outlet temperature and the absorber specific output power. The models of absorbers 1 and 2 have the lowest misrepresentation of real measured data, while the model of absorber 4 has the highest.

4.2. Efficiency curves

The presentation of test results according to the standard shall be in the form of a power curve as a function of the temperature difference - between the fluid mean temperature and the ambient temperatures ($\vartheta_m - \vartheta_a$). Those curves can be presented also as efficiency curves - at certain common (or probable) operation conditions. Efficiency curves include a lot of information about the thermal performance of the absorbers and can be used for comparison. The power is calculated from Eq. (2), using the value of $G = 1000\ W/m^2$ and $u = 3\ m/s$. A value of $(E_L - \sigma T_a^4) = -100\ W/m^2$ (which corresponds to about a clear sky condition when $\vartheta_a = 20\ °C$ and $\vartheta_{sky} = 0\ °C$) should be also used in the equation [18]. The parameter $d\vartheta/dt$ is set to zero, i.e. c_5 is not indicated in the efficiency curves [18]. The diffuse fraction of solar radiation was neglected, and normal beam radiation was assumed.

Fig. 7 shows the heating efficiency curves for the four absorbers. The heating efficiency (η_H) is expressed as the ratio of the specific useful (heating) power output of the absorber (Eq. (2)) to the incident global solar irradiance, as per Eq. (5). The efficiency is plotted against the reduced temperature difference $T^* = (\vartheta_m - \vartheta_a)/G$. Not only the heat loss coefficient (c_1) accounts for the slope of the curves, but also its wind dependence (c_3). This is because the wind speed is not neglected ($u = 3\ m/s$). The intersection value of the curves (i.e. at zero temperature difference) is a result of the combined effect of both the zero-loss efficiency ($F'(\tau\alpha)$) and its wind dependence (c_6).

$$\eta_H = \frac{\dot{Q}_N}{G_g} \tag{5}$$

Since the main focus of this research was on providing cooling, the comparison between the four absorbers should be made according to their cooling efficiency curves. Similar to the heating case, the cooling efficiency curves can be plotted, taking into consideration that no solar irradiance exists, and that the main available resource for night-cooling is the radiative cooling, i.e. the net long-wave irradiance. Accordingly, the cooling efficiency η_C is the ratio of the specific useful (cooling) power output of the absorber (Eq. (2)) to the net long-wave irradiance, as expressed below in Eq. (6):

$$\eta_C = \frac{\dot{Q}_N}{(E_L - \sigma T_a^4)} \tag{6}$$

As shown in Fig. 8, at zero temperature difference, the cooling effect is purely due to radiation. The efficiency then is equivalent to the (ε/α)-ratio - the long-wave irradiance dependence factor of the heat losses (c_4).

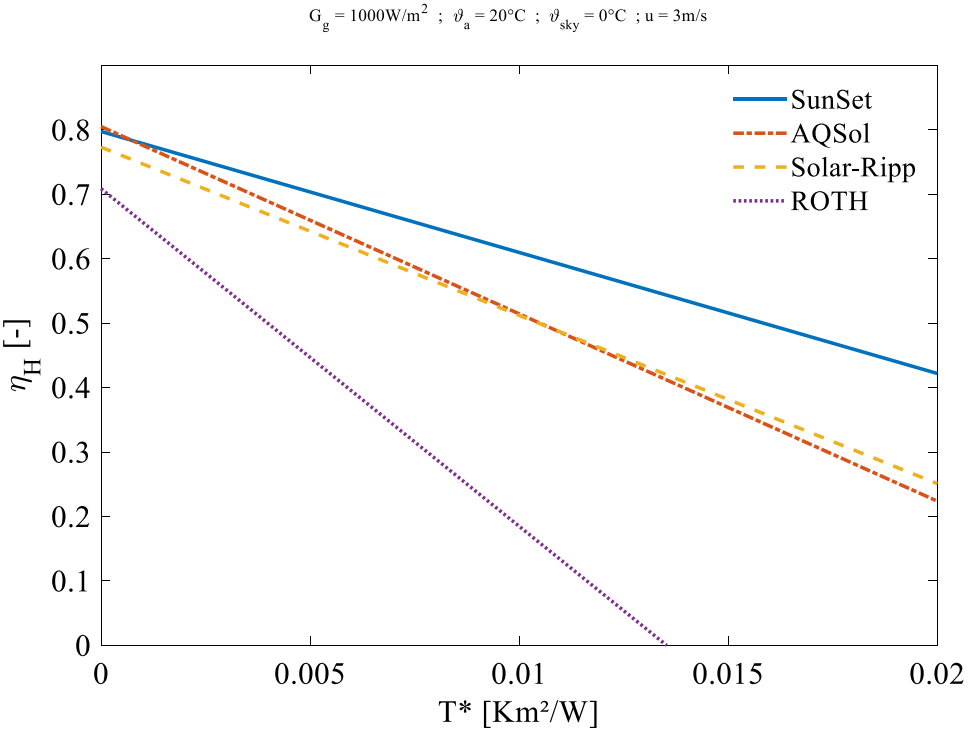

Fig. 7. Efficiency curves for heating applications of the four absorbers under testing.

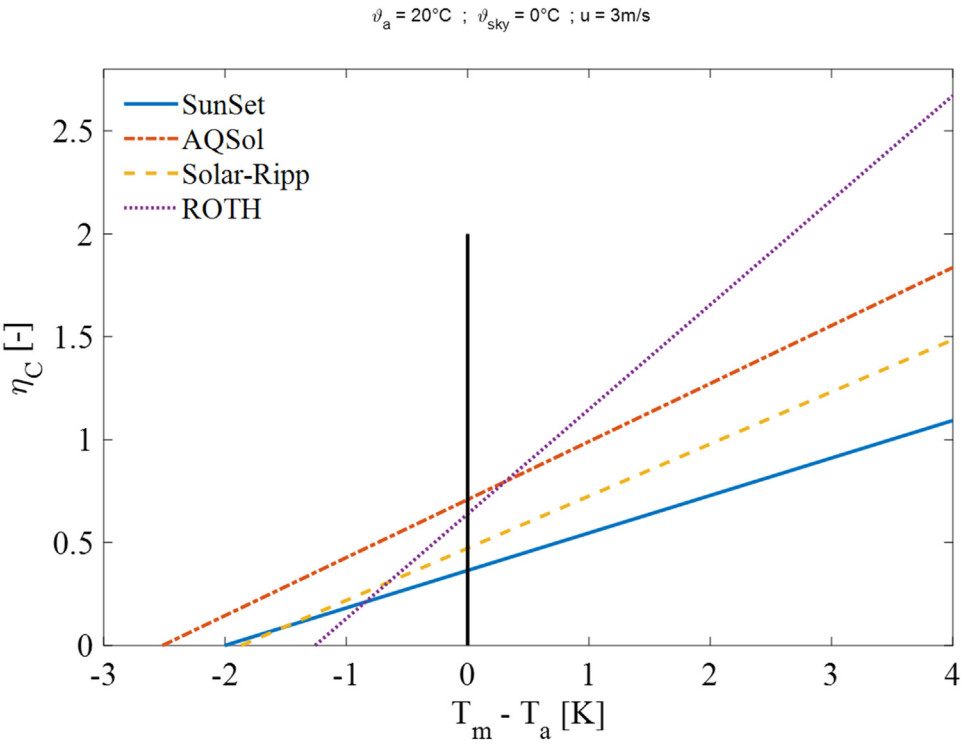

Fig. 8. Efficiency curves for cooling applications of the four absorbers under testing.

Elsewhere on the plot, the cooling effect is a mix of both radiation and convection. In contrast to the conventional way of understanding "efficiency", the cooling efficiency η_C can be greater than unity. This happens when $T_m > T_a$, where the convective heat loss assists radiative-cooling (s. Section 2.2). Since convection improves the night-cooling process in this particular case (the right-hand part of the graph), it is even called "convective gains" rather than heat loss. On the other hand, the convective effect opposes the cooling process, to the left of the zero line on the plot, as it causes heat gains. In that region of the plot (the left-hand part of the graph), it is called "convective losses". Same as previous analysis of the heating curves, the slope of the cooling efficiency curves depends on the values of the heat loss coefficient (c_1) and its wind dependence (c_3).

From the cooling efficiency curves on Fig. 8, absorber 2 (AQSol) shows the best overall thermal performance for night-cooling applications, especially at absorber mean temperatures lower than the ambient temperature. This is the case of the undesired scenario when convection is impeding radiative cooling, but it is probable to happen. On the other hand, when considering the heating applications (Fig. 7), absorber 2 is almost at the second place after absorber 1 (SunSet).

5. Conclusion & outlook

The research work summarized in this paper focused on testing four plastic solar thermal collectors. The goal was to identify their thermal performance parameters. This would enable plotting their efficiency curves and hence evaluating them thermally, in preparation for a following simulation phase. In addition to the typical heating applications, uncovered plastic STCs (solar absorbers) can be used for nocturnal radiative cooling applications. For such purposes, the complete mathematical model of the collector is mandatory. The parameter c_4 accounts for the heat loss dependence on long-wave irradiance, and it is equivalent to the (ε/α)-ratio of the collector. The datasheets provided by manufacturers do not usually include the full set of collector parameters.

The international standard EN ISO 9806 describes the quasi-dynamic test method, which is the basis for the detailed model of STCs. The available version of the standard at the time of conducting this work (ISO 9806:2013) was followed to test the four absorbers. An updated version of the standard was introduced after the completion of this research-work. The ISO 9806:2017 carefully considered the various types and applications of solar collectors, e.g. PVTs, swimming-pool, façade integrated, and concentrating collectors. An expanded mathematical model (with two more heat loss coefficients) was accordingly introduced to better describe the thermal performance of STCs. An overview of this latest version of the standard is presented in this guide [28]. By definition, standards undergo a critical review and revision about every 5 years. In May 2022, the technical committee formally registered the following revision to release a newer version of the ISO 9806 that was last issued in 2017. The draft is planned to be ready by the end of 2023. And the newest update is expected to be published in 2024. In the awaited new version of the ISO 9806, it is being considered to include nighttime tests and tests below ambient temperature [21].

For the outdoors testing, a suitable test-stand equipped with all needed measurement devices was available. The test set-up also offered simultaneous testing of the four absorbers, which allowed undergoing same testing conditions. The ISO 9806:2013 recommended specific (yet various) weather conditions for the test period. Because of the time-frame of the project's phases, the test days in this work were not fully complying with the required conditions. This might affect the quality of the results. It is therefore highly recommended to check the requirements of such outdoors tests in advance. And based on the weather conditions at the test-site, the testing phase should be scheduled. The test data were used in an optimization template in TRNSYS17, where the full set of coefficients of the dynamic model of an unglazed solar collector (Type1289) were parameterized. An updated collector model (Type1287) has been available since December 2021, which allows for the introduction of the additional heat loss coefficients as adopted in the newest ISO 9806:2017. In an optimization process for those parameters, GenOpt was coupled with this simulation model to eventually identify the parameters of each absorber. The complete set of parameters for each absorber could be identified. Only the coefficient c_6 (the wind dependence of the zero-loss efficiency) for three absorbers were set to its predefined minimum limit. That was not crucial for the (nocturnal) cooling efficiency curves.

The overall validation results were good. The first two absorbers had the lowest misrepresentation versus real measured data, while the model of the third tested absorber had the highest. The standard deviation (between simulated and measured values) of the fluid outlet temperature was 0.37, 0.39 and 0.67 ˚C, respectively. Whereas, it was 38.79, 50.82 and 77.22 W/m^2 for the specific output power. The values of the fourth tested absorber were in between. The heating and cooling efficiency curves were plotted for the four absorbers using the identified parameters. As recommended by the standard, these values were used for plotting the curves: $\vartheta_a = 20\ °C, \vartheta_{sky} = 0\ °C,\ u = 3\ m/s$, and $G = 1000\ W/m^2$ (the latter is needed for the heating case only). From the two efficiency curves, absorber 2 showed the optimum performance for combined heating and cooling applications. It was therefore selected to simulate the unit of an uncovered plastic solar collector field in a following phase of this research-project.

In the past few years, there has been a sound research on the topic of radiative cooling. The recent research focused however on daytime radiative cooling. Modern technologies are considered for different materials to improve their performance for radiative cooling. Innovative application areas are also tackled. An academic work that correlates the main outcomes of these different research areas would represent a roadmap for remarkable research in this promising topic.

Declaration of Competing Interest

The authors declare that they have no known competing financial interests or personal relationships that could have appeared to influence the work reported in this paper.

Acknowledgment

This paper is an updated summary of the first part of a master-thesis submitted in November 2016 to Faculty 5/Institute of Physics at the University of Oldenburg. The work was carried out at the Hochschule für Technik Stuttgart (HFT-Stuttgart) in the context of the research project NightCool, funded by the German Federal Ministry of Education and Research (BMBF). Support code: 01DH14021. The project was followed by a second-phase project, PVT-RESyst (support code: 01DG18002), for demonstration & concept realization, which ended in February 2021. Many thanks to everyone who contributed, on all levels, to make this work happen.

Supplementary materials

Supplementary material associated with this article can be found, in the online version, at doi:10.1016/j.seja.2023.100038.

References

[1] D.S. Parker, J.R. Sherwin, A.H. Hermelink, NightCool: A Nocturnal Radiation Cooling Concept, in: ACEEE Summer Study on Energy Efficiency in Buildings, 2008, pp. 209–222.
[2] M. Santamouris, Advances in Passive Cooling, Earthscan, London, 2007.
[3] M.A. Al-Nimr, Z. Kodah, B. Nassar, A theoretical and experimental investigation of a radiative cooling system, Sol. Energy 63 (6) (1998) 367–373.
[4] A.H.H. Ali, Passive cooling of water at night in uninsulated open tank in hot arid areas, Energy Convers. Manag. 48 (1) (2007) 93–100.
[5] X. Lu, P. Xu, H. Wang, T. Yang, J. Hou, Cooling potential and applications prospects of passive radiative cooling in buildings: the current state-of-the-art, Renew. Sustain. Energy Rev. 65 (2016) 1079–1097.
[6] S. Vall, A. Castell, Radiative cooling as low-grade energy source: a literature review, Renew. Sustain. Energy Rev. 77 (2017) 803–820 January, doi:10.1016/j.rser.2017.04.010.
[7] M. Zeyghami, D.Y. Goswami, E. Stefanakos, A review of clear sky radiative cooling developments and applications in renewable power systems and passive building cooling, Sol. Energy Mater. Sol. Cells 178 (2018) 115–128 January, doi:10.1016/j.solmat.2018.01.015.
[8] J. Chen, L. Lu, Development of radiative cooling and its integration with buildings: a comprehensive review, Sol. Energy 212 (2020) 125–151 November, doi:10.1016/j.solener.2020.10.013.
[9] U. Eicker, A. Dalibard, Photovoltaic-thermal collectors for night radiative cooling of buildings, Sol. Energy 85 (7) (2011) 1322–1335.
[10] X. Yu, C. Chen, A simulation study for comparing the cooling performance of different daytime radiative cooling materials, Sol. Energy Mater. Sol. Cells 209 (2020) 110459 January, doi:10.1016/j.solmat.2020.110459.
[11] J. Zhang, et al., A flexible film to block solar radiation for daytime radiative cooling, Sol. Energy Mater. Sol. Cells 225 (2021) 111029 February, doi:10.1016/j.solmat.2021.111029.
[12] K. Te Lin, J. Han, K. Li, C. Guo, H. Lin, B. Jia, Radiative cooling: fundamental physics, atmospheric influences, materials and structural engineering, applications and beyond, Nano Energy 80 (2021) July 2020, doi:10.1016/j.nanoen.2020.105517.
[13] E. Erell, Y. Etzion, Radiative cooling of buildings with flat-plate solar collectors, Build. Environ. 35 (4) (2000) 297–305.
[14] A. Hamza, I.M.S. Taha, I.M. Ismail, Cooling of water flowing through a night sky radiator, Sol. Energy 55 (4) (1995) 235–253.
[15] M. Al-Nimr, M. Tahat, M. Al-Rashdan, A night cold storage system enhanced by radiative cooling - a modified Australian cooling system, Appl. Therm. Eng. 19 (1999) 1013–1026.
[16] X. Jobard, R. Braun, J. Cremers, U. Eicker, N. Palla, Experimental performance analysis of innovative uncovered PV-T collectors for radiative cooling and heating applications xavier, in: Proceedings of the EuroSun (ISES Conference Proceedings), 2014.
[17] S. Fischer et al., Collector test method under quasi-dynamic conditions according to the European Standard EN 12975-2, in ISES Solar World Congress, 2001, pp. 1–8.
[18] ISO 9806, Solar energy – Solar thermal collectors – Test methods. The International Organization for Standardization, 2013.
[19] DIN EN ISO 9806, Solarenergie – Thermische Sonnenkollektoren – Prüfverfahren (German version EN ISO 9806:2017). DEUTSCHE NORM, pp. 1–107, 2018.
[20] Peter Kovacs et al., A GUIDE TO THE STANDARD EN12975 - Quality Assurance in Solar Heating and Cooling Technology. QAiST - IEE/08/593/SI2.529236, Deliverable D2.3, pp. 1–80, 2012.
[21] S. Fischer, Global Solar Certification Network and SOLERGY. IEA SHC Solar Academy Webinar, 2023, [Online]. Available at: https://www.iea-shc.org/solar-academy/webinar/global-solar-certification-network-and-solergy.
[22] J.A. Duffie, W.A. Beckman, Solar Engineering of Thermal Processes, John Wiley & Sons, New York, 1991.
[23] S. Ahmed, Z. Li, M.S. Javed, T. Ma, A review on the integration of radiative cooling and solar energy harvesting, Mater. Today Energy 21 (2021) 100776, doi:10.1016/j.mtener.2021.100776.
[24] K. Zelzouli, A. Guizani, R. Sebai, C. Kerkeni, Solar thermal systems performances versus flat plate solar collectors connected in series, Engineering 04 (2012) 881–893, doi:10.4236/eng.2012.412112.
[25] Operating instructions for handling ethylene glycol (Betriebsanweisung für den Umgang mit Ethylenglykol). HFT-Stuttgart/Mechanische Werkstatt, pp. 1–4, 2016.
[26] M. Wetter, GenOpt - a generic optimization program, in: Proceedings of the Seventh International IBPSA Conference, IBPSA's Building Simulation, Rio de Janeiro, 2001.
[27] "TESSLibs 17 - Solar Library Mathematical Reference (Vol. 10)," in Component Libraries for the TRNSYS Simulation Environment, TESS Thermal Energy Systems Specialists, 2012, p. 165.
[28] K. Kramer et al., Guide to the standard ISO 9806:2017 (A Resource for Manufacturers, Testing Laboratories, Certification Bodies and Regulatory Agencies). Fraunhofer ISE, pp. 1–66, 2017, doi:10.13140/RG.2.2.27725.08168.